

---

# Effective Verdet Constant in Terbium-Doped-Core Phosphate Fiber

Faraday rotators are widely used in optical isolators, circulators, Faraday mirrors, and magnetic/current field sensors. Traditional Faraday rotators are based on bulk optics, which require optical coupling for use with fiber-optic systems. Optical fibers continue to be the platform of choice in many optics fields, making the development of all-fiber Faraday rotation components highly desirable. This is particularly true for high-power fiber laser systems, where fiber termination and small free-space beams place restrictions on how much power can be transported through such components in order to avoid damage at optical interfaces.

Several standard silica-fiber Faraday rotators have been reported<sup>1-4</sup> but are relatively impractical because of long fiber lengths. The small Verdet constant in standard silica fiber, which translates to a long fiber length, makes it difficult to realize all-fiber Faraday rotators. The Verdet constant is only about 1 rad/Tm at 1064 nm in silica, compared with 40 rad/Tm in terbium gallium garnet (TGG) crystals often used in bulk optics.<sup>5</sup> As an example, if the magnetic field is 0.2 T, the silica fiber length required for a 45° rotation is around 4 m. To maintain a constant orientation of the magnetic field along the entire axial length, the fiber cannot be coiled. This creates an impractical requirement that the magnet structure be as long as the fiber.

To overcome this limitation, Shiraishi<sup>6</sup> reported the fabrication of a high-Verdet-constant (21× greater than silica fiber) optical fiber using Hoya FR-5 (terbium borosilicate) glass, where both the core and the cladding were doped with terbium (Tb). Ballato and Snitzer<sup>7</sup> also reported the fabrication of a 54-wt%-terbium-doped optical fiber, measuring the Verdet constant on bulk samples to be 20× higher than silica fiber.

Doping with high-Verdet-constant materials, such as terbium, can be an effective way to increase the total Verdet constant in optical fiber. The Verdet constant experienced by an optical field is different, however, from the material Verdet constants in the core and cladding when they are made of different materials. The results described above did not measure or

predict this effect. The first experimental proof of the effective Verdet constant theory is presented in this article. The effective Verdet constant in a phosphate fiber that is terbium doped in the core only is measured. The experimental results agree well with theory and describe how the effective Verdet constant differs from the value measured from the bulk samples.

The Verdet constant experienced by light in an optical fiber is different from that in bulk glass. In bulk glass, the Verdet constant is normally uniform everywhere. In optical fiber, the core and cladding have different Verdet constants since they are typically made of different materials. Only a portion of the guided mode exists in the core of the fiber waveguide. Thus, the effective Verdet constant  $V_{\text{eff}}$  is defined as the Verdet constant experienced by the optical mode in the fiber,

$$V_{\text{eff}} = V_{\text{core}}\Gamma + V_{\text{clad}}(1 - \Gamma), \quad (1)$$

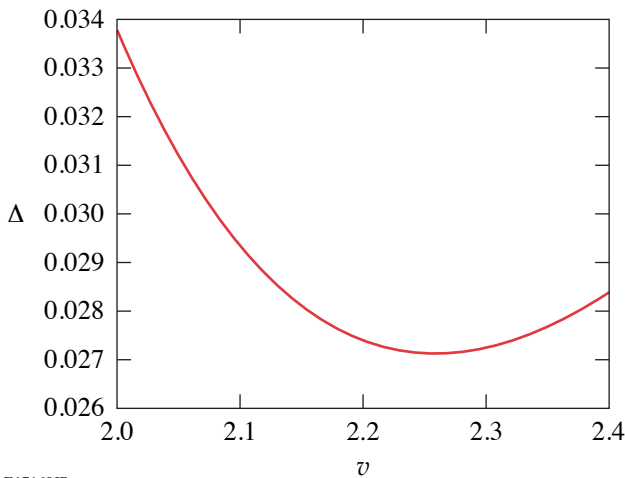
where  $V_{\text{core}}$  and  $V_{\text{clad}}$  are the Verdet constants in the core and cladding, respectively, and the confinement factor  $\Gamma = P_{\text{core}}/P_{\text{tot}}$  represents the ratio of the power contained in the core,  $P_{\text{core}}$ , to total power  $P_{\text{tot}}$ . The confinement factor  $\Gamma$  can be calculated directly by assuming that the fundamental mode profile is Gaussian,  $\Gamma = 1 - \exp(-2/\xi^2)$ . The ratio of beam-spot size to fiber radius  $\xi$  is usually approximated by

$$\xi \approx 0.65 + 1.619 v^{-3/2} + 2.879 v^{-6}, \quad (2)$$

which is accurate to within 1% for  $1.2 \leq v \leq 2.4$ , where  $v$  is the normalized frequency (or  $V$  number).<sup>8</sup> Equation (1) for the effective Verdet constant has a straightforward physical meaning: the Verdet constant includes two parts contributing from the core and the cladding, weighted by the mode overlap in each region.

In recent theoretical work,<sup>9</sup> the rotation of an optical field in a fiber was derived using Maxwell's equations with a magnetic field applied along the axial direction of the fiber. An empirical equation, which has a relative error of 2% for  $1 \leq v \leq 3$ , was used to approximate the propagation constant. Using these results,

one can derive the effective Verdet constant directly from the circular birefringence of the propagation constant. After algebraic manipulation, this derivation produces an effective Verdet constant given by  $V_{\text{eff}}^{\text{Yoshino}} = V_{\text{core}}\alpha + V_{\text{clad}}(1 + \alpha)$ , where the factor  $\alpha = 1.306 - 1.138/v$  and is a dimensionless constant. Figure 117.46 shows the relative difference  $\Delta = (\alpha - \Gamma)/\alpha$  between factors  $\Gamma$  and  $\alpha$  as a function of normalized frequency  $v$ . In the region  $2 < v < 2.4$ , where most single-mode fibers are designed,  $\Delta$  is less than 4%. Considering that both models use empirical equations during derivation, such a difference is reasonable. Therefore, although not indicated in Ref. 9, the factor  $\alpha$  should have the same physical meaning as  $\Gamma$ , representing the light confinement in the core. This indicates that Eq. (1) can also be derived via rigorous electromagnetic calculations.



E17160JR

Figure 117.46 Normalized difference between factors  $\Gamma$  and  $\alpha$  for a single-mode fiber as a function of normalized frequency  $v$ .

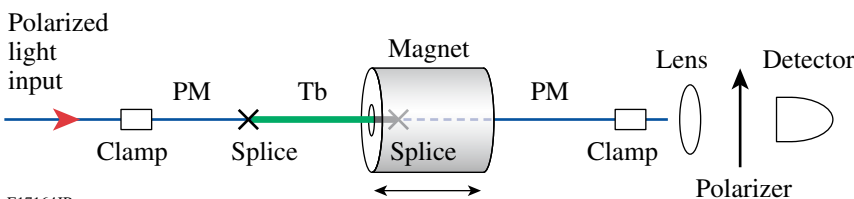
The phosphate optical fiber used in these experiments was fabricated at NP Photonics.<sup>10</sup> It is 25-wt% terbium doped in the single-mode core [numerical aperture (N.A.) = 0.147] and 6-wt% lanthanum doped in the cladding to provide the appropriate core N.A. Core and cladding diameters are  $4.5 \mu\text{m}$  and  $120 \mu\text{m}$ , respectively, and the propagation loss is 0.12 dB/cm

at 980 nm. The Verdet constant is measured at 1053 nm and room temperature using the experimental configuration shown in Fig. 117.47. A 4-cm section of Tb-doped phosphate fiber, spliced between two polarization-maintaining (PM) fibers, goes through a magnet tube. Linearly polarized, 1053-nm light is launched into the fiber, and the polarization direction of the output light is monitored. The N48 NdFeB magnet tube is 4 cm long with inner and outer diameters of 5 mm and 6 cm, respectively. As the magnet is translated along the fiber, the magnetic field imposed on the Tb fiber is changed. By measuring the rotation angle as a function of the magnet's position on the fiber axis,  $V_{\text{eff}}$  can be extracted, provided the magnetic field is known.

Magnetic fields can be readily calculated by using the geometrical shape of the magnet.<sup>11</sup> The axial component of the magnetic-field distribution along the central axis of the magnet tube is derived to be

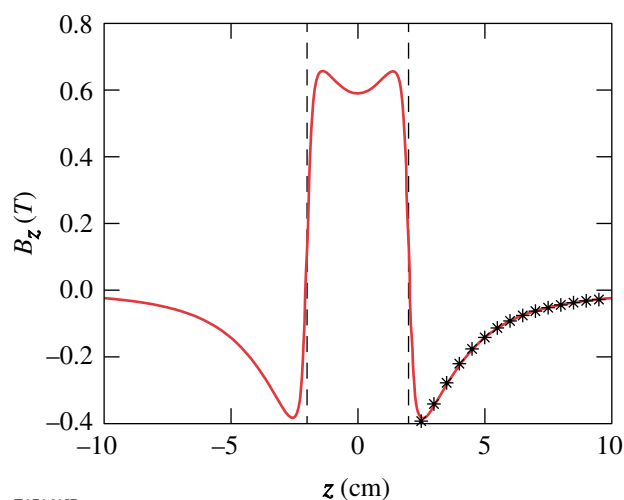
$$B_z(z) = \frac{B_r}{2} \left\{ \frac{z+l/2}{\left[ a_1^2 + (z+l/2)^2 \right]^{1/2}} - \frac{z+l/2}{\left[ a_2^2 + (z+l/2)^2 \right]^{1/2}} - \frac{z-l/2}{\left[ a_1^2 + (z-l/2)^2 \right]^{1/2}} + \frac{z-l/2}{\left[ a_2^2 + (z-l/2)^2 \right]^{1/2}} \right\}, \quad (3)$$

where  $a_1$  and  $a_2$  are the inner and outer radii, respectively,  $l$  is the length of the magnet, and  $B_r$  is the residual magnetic flux density. Figure 117.48 shows the calculated  $B_z(z)$  for the N48 magnet used in the experiment ( $B_r = 1.35T$ ) along with the measured magnetic field outside the magnet. The physical ends of the magnet are also shown for reference. The magnetic field, measured only outside the magnet because the probe size is larger than  $a_1$ , agrees very well with the theoretical curve calculated from Eq. (3). The magnetic field has different directions inside and outside the magnet, such that the total integrated field along the  $z$  axis is zero, i.e.,  $\int_{-\infty}^{+\infty} B_z(z) dz = 0$ , resulting from Ampère's law. This means that if a sufficiently long piece of fiber with axially uniform  $V_{\text{eff}}$  goes through the



E17164JR

Figure 117.47 Experimental configuration of the Faraday rotation measurement.



E17161JR

Figure 117.48

Theoretical (solid) and measured (star) magnetic density flux distribution  $B_z$  along the center axis  $z$ ; dashed lines represent the magnet ends.

magnet, the rotation angles inside and outside the magnet counteract each other and the total rotation angle is zero. If the fiber consists of  $i$  different sections of length  $L_i$ , the total rotation angle  $\Delta\theta_{\text{tot}}$  can be written as a sum of the rotation in each section  $\Delta\theta_i$ , given by

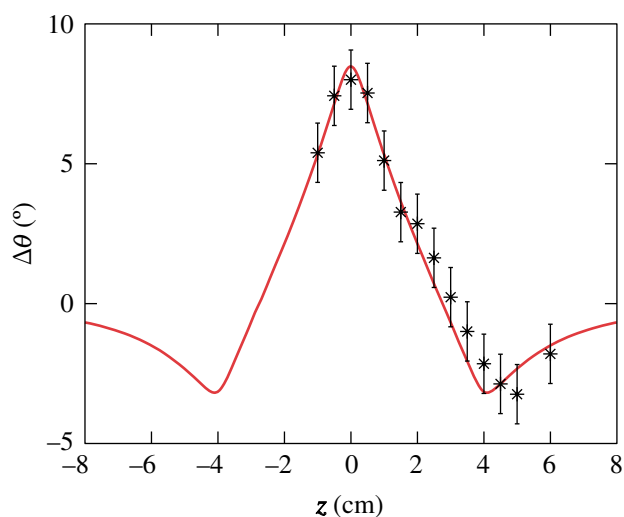
$$\Delta\theta_{\text{tot}} = \sum_i \Delta\theta_i = \sum_i V_{\text{eff}}^i \int_{L_i} B_z(z) dz, \quad (4)$$

where  $V_{\text{eff}}^i$  and  $\int_{L_i} B_z(z) dz$  are the effective Verdet constant and the line integral of the magnetic field in each section, respectively. For the experimental configuration shown in Fig. 117.47, Eq. (4) can be simplified as

$$\Delta\theta_{\text{tot}} = V_{\text{eff}}^{\text{Tb}} \int_{L_{\text{Tb}}} B_z(z) dz + V_{\text{eff}}^{\text{PM}} \int_{L_{\text{PM}}} B_z(z) dz, \quad (5)$$

where the two terms represent the Verdet constant of and the integration over the Tb-doped and PM fibers, respectively.  $V_{\text{eff}}^{\text{PM}}$  can be neglected in our experiment because the large linear birefringence in PM fiber suppresses Faraday rotation.

In the experiment, the magnet is axially translated in 5-mm steps. At each step, the direction of the major polarization axis is measured; the power is measured as the polarizer in front of the detector is rotated, and the polarization direction is extracted by fitting this data to a cosine-squared function. Figure 117.49 shows the measured rotation angle and the corresponding curve fit at 1053 nm along the central axis. The error



E17165JR

Figure 117.49

Measured (star) rotation angle and corresponding curve fit (solid) at 1053 nm along the center axis  $z$ .

in the measured angle is primarily caused by air flow, and it is determined to be  $1^\circ$  by a polarization stability measurement. The curve fit is obtained by adjusting  $V_{\text{eff}}^{\text{Tb}}$ , yielding a measured Verdet constant of  $V_{\text{measure}} = -6.2 \pm 0.4$  rad/Tm. This value is  $6\times$  higher than that of the silica and demonstrates the potential for compact all-fiber Faraday rotators.

The bulk value of the Tb-doped core is calculated from Ref. 7 to be  $V_{\text{core}} = -9.3$  rad/Tm, assuming a linear dependence on the terbium ion concentration. Since no Verdet constant data are available in the near-infrared region for the lanthanum-doped phosphate glass used in the cladding, the value is approximated based on two observations: First, the Verdet constant dispersion curve of the lanthanum-doped phosphate glass is roughly 0.8 rad/Tm higher than the curve for  $\text{SiO}_2$  in the visible region.<sup>12,13</sup> Assuming a similar trend in the near-infrared region, the Verdet constant of the lanthanum-doped phosphate glass should be 0.8 rad/Tm larger than that of the  $\text{SiO}_2$ . Second, the rare-earth element present in the host material is the dominating factor in determining the Verdet constant. For example, the Verdet constant of the terbium aluminosilicate is similar to that of the terbium phosphate.<sup>13</sup> Therefore, the Verdet constant of the crystal lanthanum fluoride ( $\text{LaF}_3$ ) measured at 1064 nm (Ref. 12) should also be similar to that of lanthanum phosphate. Both of these observations lead to a value of  $V_{\text{clad}} = 1.8$  rad/Tm. Using these values for the core and cladding Verdet constants, the theoretical models predict  $V_{\text{eff}} = -6.0$  rad/Tm and  $V_{\text{eff}}^{\text{Yoshino}} = -6.3$  rad/Tm, the differ-

ence between the models resulting from the approximations contained in each. They both agree well with the experimental result, which differs substantially from the bulk core value of  $-9.3$  rad/Tm due to the mode confinement properties of the fiber, as described above. This measurement validates the theory of the effective Verdet constant.

Several methods can be used to increase the effective Verdet constant for compact all-fiber Faraday rotators. For example, the same high-Verdet-constant material can be doped in both the core and the cladding. In this case, the  $V_{\text{eff}}$  will be equal to the material's Verdet constant. If the high-Verdet-constant material is doped only in the core, the N.A. and the core diameter can be increased (while maintaining a  $V$  number less than 2.405) to confine more light in the core, therefore increasing  $V_{\text{eff}}$ . Other rare-earth elements besides terbium can also be doped. For example, praseodymium and dysprosium also have Verdet constants much higher than silica.

In conclusion, the first experimental validation of the effective Verdet constant theory has been reported. The effective Verdet constant of light propagation in a fiber includes contributions from the materials in both the core and the cladding. It is measured in a 25-wt%-terbium-doped-core phosphate fiber to be  $-6.2 \pm 0.4$  rad/Tm at 1053 nm, which is  $6\times$  larger than silica fiber. The result agrees well with the Faraday rotation theory in optical fibers.

#### ACKNOWLEDGMENT

This work was supported by the U.S. Department of Energy Office of Inertial Confinement Fusion under Cooperative Agreement No. DE-FC52-08NA28302, the University of Rochester, and the New York State Energy Research and Development Authority. The support of DOE does not constitute an endorsement by DOE of the views expressed in this article.

#### REFERENCES

1. E. H. Turner and R. H. Stolen, *Opt. Lett.* **6**, 322 (1981).
2. G. W. Day *et al.*, *Opt. Lett.* **7**, 238 (1982).
3. J.-F. Lafortune and R. Vallée, *Opt. Commun.* **86**, 497 (1991).
4. V. Annovazzi-Lodi, S. Merlo, and A. Leona, *J. Lightwave Technol.* **13**, 2349 (1995).
5. E. Khazanov *et al.*, *Appl. Opt.* **41**, 483 (2002).
6. K. Shiraiishi, S. Sugaya, and S. Kawakami, *Appl. Opt.* **23**, 1103 (1984).
7. J. Ballato and E. Snitzer, *Appl. Opt.* **34**, 6848 (1995).
8. G. P. Agrawal, *Lightwave Technology: Components and Devices* (Wiley, Hoboken, NJ, 2004).
9. T. Yoshino, *J. Opt. Soc. Am. B* **22**, 1856 (2005).
10. NP Photonics, Inc., Tucson, AZ 85747, <http://www.npphotonics.com>.
11. M. McCaig and A. G. Clegg, *Permanent Magnets in Theory and Practice*, 2nd ed. (Wiley, New York, 1987).
12. D. R. Lide, *CRC Handbook of Chemistry and Physics*, 82nd ed. (CRC Press, Boca Raton, FL, 2001).
13. M. J. Weber ed., *CRC Handbook of Laser Science and Technology*, edited by M. J. Weber, Supplement 2: Optical Materials (CRC Press, Boca Raton, FL, 1995), Sec. 9.